

Electronic Structure of Amorphous SiO_x with Variable Composition

A. A. Karpushin^{a,*} and V. A. Gritsenko^{a, b, c}

^a Rzhanov Institute of Semiconductor Physics, Siberian Branch, Russian Academy of Sciences,
Novosibirsk, 630090 Russia

^b Novosibirsk National Research State University, Novosibirsk, 630090 Russia

^c Novosibirsk State Technical University, Novosibirsk, 630073 Russia

*e-mail: tomakarp@yahoo.com

Received March 20, 2018; in final form, June 20, 2018

The heights of barriers for the injection of electrons and holes from silicon in SiO_x have been calculated in the tight binding approximation without any fitting parameters. The dependence of the electronic structure of silicon-enriched amorphous silicon oxide SiO_x on the degree of enrichment has been found. The calculations have been performed with the parameterization of the matrix elements of the tight binding Hamiltonian proposed in our previous work. This parameter involves a change in the localization region of valence electrons of an isolated atom at its introduction into a solid. It has been shown that the inclusion of this change makes it possible to calculate the electronic structure without fitting parameters using the parameters of individual atoms as initial data. This circumstance allows the calculation in the absolute energy scale with zero corresponding to the energy of the electron in vacuum.

DOI: 10.1134/S0021364018140084

Silicon oxide is one of the key insulators in technology and design of silicon devices [1, 2]. New interest in SiO_x is stimulated by the development of high-speed resistive flash memory of a new generation [3–5]. A resistive memory effect was discovered in non-stoichiometric silicon oxide SiO_x at $x \leq 2$. This effect means that its resistance varies exponentially at the application of a voltage and the resistance does not change in time [6]. Resistive flash memory can have a response time of 1 ns, which is seven orders of magnitude smaller than a response time of 10 ms of currently dominant commercial memory based on silicon nitride. Furthermore, resistive memory can withstand 10^{12} programming cycles as compared to 10^4 cycles for memory based on silicon nitride. All these circumstances stimulate a rapid increase in the number of studies of nonstoichiometric silicon oxide [7–9].

A key unsolved problem in the physics of the resistive memory effect in SiO_x is understanding of mechanisms of charge transport (electrons and holes) through an insulator. The probability of the injection of electrons and holes from a contact to the insulator depends exponentially on the barrier height at the contact–insulator interface [10, 11]. To date, only a qualitative theory of the dependence of the width of the band gap on the composition of SiO_x has been developed [12, 13]. However, the interpretation of experiments on the charge transport in a resistive flash memory cell based on SiO_x requires quantitative data

on the heights of the electron and hole barriers on contacts.

This circumstance imposes certain requirements on the calculation method. In particular, ab initio density functional theory calculations underestimate the width of the band gap of the insulator. For example, the width of the band gap E_g of Ta_2O_5 is 1.3 eV [14, 15], whereas E_g for various modifications of HfO_2 lies in the range of 3.2–3.8 eV [16], and the experimental E_g value is 4.2 eV for Ta_2O_5 [12] and 5.6 eV for HfO_2 [1]. Cluster quantum chemical methods are also inappropriate for these calculations because of quantum confinement effects.

Band calculation methods cannot be used to calculate the electronic structure of amorphous solids because translational symmetry is absent in them. It is noteworthy that the feature of SiO_x is a compositional disorder caused by a random substitution of silicon atoms for four oxygen atoms in a SiO_4 tetrahedron. This disorder can be described within the Bethe lattice model. For this reason, to calculate the electronic structure of SiO_x with a variable composition, we used the ab initio tight binding method with the generalized Bethe lattice model proposed in [17] as a structural model. Such method and model were chosen because their application in our previous calculations of the electronic structure of broadband insulators SiO_xN_y [18] and SiN_x [19–21] with variable composition gave

the positions of the edges of the band gap in good agreement with experimental data.

We calculate the electronic structure of SiO_x in terms of the local density of states at sites of the lattice of the insulator. Such a calculation gives not only the form of the electronic structure but also the partial contribution of atomic states to the features of this structure. The method used in this calculation was described in detail in [18–21]. The local density of states at sites of the lattice is given by the expression

$$N_{i\alpha} = -\frac{1}{\pi} \text{Im}(G_{i\alpha,i\alpha}),$$

where $G_{i\alpha,i\alpha}(E + i0)$ is the diagonal matrix element of the one-electron Green's function, which is the solution of the system of equations

$$\sum_{l,\gamma} [(E + i0)\delta_{i,l}\delta_{\alpha,\gamma} - H_{i\alpha,l\gamma}]G_{l\gamma,j\beta}(E + i0) = \delta_{ij}\delta_{\alpha\beta}. \quad (1)$$

Here, Latin subscripts specify the positions of atoms in the lattice, Greek subscripts enumerate atomic orbitals, and $H_{i\alpha,l\gamma}$ are the matrix elements of the tight-binding Hamiltonian in the site representation:

$$\hat{H} = \sum_{i\alpha} E_{i\alpha} \hat{c}_{i\alpha}^+ \hat{c}_{i\alpha} + \sum_{j\beta} V_{i\alpha,j\beta} \hat{c}_{i\beta}^+ \hat{c}_{i\beta} + \text{H.c.} \quad (2)$$

The determination of the matrix elements of the tight-binding Hamiltonian is the most important for the calculation of the local electronic structure. In the simplest variant of the tight-binding method, the diagonal matrix elements of the tight-binding Hamiltonian $H_{i\alpha,i\alpha}$ are taken to be the energy of the atomic level of the α th orbital of the i th atom in an insulated state. The off-diagonal matrix elements are accepted to be proportional to the overlap integrals of the orbitals of neighboring atoms in the lattice. This variant disregards charge transfer between atoms in the crystal, which occurs in ionic and ionic covalent crystals. A change in the localization region of valence electrons at the introduction of individual atoms in the crystal is also ignored. As will be shown below, charge transfer and the change in the localization region of valence electrons of atoms of a solid significantly affect the matrix elements of the tight-binding Hamiltonian. It is noteworthy that charge transfer was taken into account in [22, 23] by introducing an intraatomic Coulomb correlation proportional to the transferred charge. However, it was disregarded that a change in the charge state changes the localization region of introduced atoms and that the interatomic distance in a solid is not the sum of covalent radii of atoms composing the insulator. For this reason, corrections proposed in [22, 23] did not provide quantitative agreement between the calculated electronic structure and experimental data. For agreement between the calculation and experimental data, Harrison [23] had to fit matrix elements of the tight-binding

Hamiltonian to the experimental result, which reduced the predictive validity of these calculations.

In this work, we take into account changes in the localization region of valence electrons of silicon and oxygen at the introduction of their atoms in SiO_x . The corresponding changes in the intra-atomic potential energy of valence electrons and their kinetic energy, as well as in the matrix elements of the tight-binding Hamiltonian for SiO_x , are calculated. In particular, the diagonal matrix element $H_{i\alpha,i\alpha} = E_{i\alpha}$ for the i th site with the α th type of wavefunction can be represented in the form

$$H_{i\alpha,i\alpha} = H_{i\alpha,i\alpha}^0 + U_{i\alpha} - T_{i\alpha}, \quad (3)$$

where $H_{i\alpha,i\alpha}^0$ is the diagonal matrix element of the individual atom, $T_{i\alpha}$ is the change in the intra-atomic kinetic energy, and $U_{i\alpha}$ is the additional Coulomb repulsion caused by the change in the localization region of valence electrons at the formation of the solid. These changes can be represented in the form

$$T_{i\alpha} = T_{i\alpha}^0 \left(\frac{a_i^0}{a_i} \right)^2, \quad U_{i\alpha} = U_{i\alpha}^0 \left(\frac{a_i^0}{a_i} \right). \quad (4)$$

Here, $T_{i\alpha}^0 = \frac{\hbar^2}{2m(a_i^0)^2}$ and $U_{i\alpha}^0$ are the parameters of individual atoms, a_i^0 is the radius of the i th atom in the isolated state, a_i is the ionic radius of this atom with a charge corresponding to its charge state in the solid. Below, we use a quadratic interpolation of the dependence of the radius of the atom on its charge state,

$$\tilde{a}_i = a_i^0 + k_{1i}\delta N_i + k_{2i}\delta N_i^2. \quad (5)$$

Here, $\delta N_i = N_i - N_i^0$ is the change in the number of electrons in the i th atom at its introduction into a solid, $N_i = \sum_\alpha n_{i\alpha}$, and the coefficients k_{1i} and k_{2i} are obtained by the extrapolation of the ionic radii of atoms to fractional charges.

The off-diagonal matrix elements $H_{i\alpha,j\beta}$ are linear combinations of two-center parameters. Expressions for two-center parameters were given in [23] and are not presented here because they are lengthy. For the calculation, we use the following formula proposed in [18]:

$$V_{i\alpha,j\beta} = \pm \sqrt{T_{i\alpha} T_{j\beta} n_{i\alpha} n_{j\beta}}, \quad (6)$$

where

$$n_{i\alpha} = \int_{-\infty}^{E_F} -\frac{1}{\pi} \text{Im}(G_{i\alpha,i\alpha}) dE. \quad (7)$$

Under this definition, the diagonal and off-diagonal matrix elements depend on the atomic levels of the initial atoms and their local coordination in the lattice

Table 1. Radii of silicon and oxygen ions in different charge states

Ion	(-3e)	(-2e)	(0)	(+4e)	(+5e)
$a_i(\text{Si})$	1.98	—	1.17	0.39	—
$a_i(\text{O})$		1.32	0.75	—	0.15

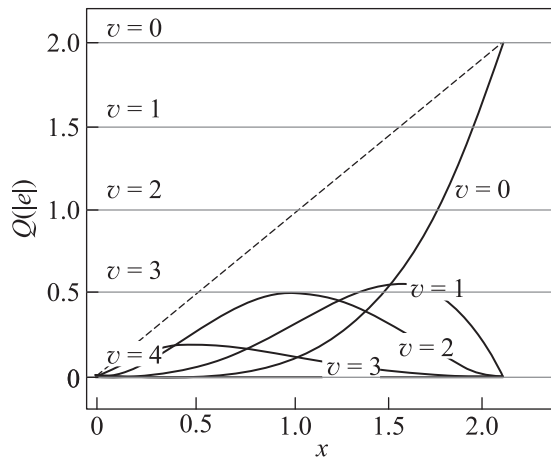
through the occupation numbers and should be determined self-consistently.

The initial atomic and ionic radii taken from [24] are presented in Table 1. As seen in Table 1, the radius of the introduced atom depends noticeably on its charge state and should also be determined self-consistently. Since the distance between atoms in a solid is not the sum of ionic radii determined by Eq. (6), we additionally scaled the radii found for Si and O atoms introduced into silicon oxide according to the expression

$$a_i = \tilde{a}_i \frac{d}{a_{\text{Si}} + a_{\text{O}}}. \quad (8)$$

The diagonal matrix elements of the Hamiltonian of individual Si and O atoms H_s^0 , H_p^0 , and $H_{s^*}^0$ and those for introduced into silicon oxide H_s , H_p , and H_{s^*} are presented in Table 2. The intra-atomic Coulomb repulsion taken from [13] is 7.64 and 13.15 eV for silicon and oxygen, respectively.

Amorphous SiO_x can be considered as a continuous chain of silicon atoms randomly bonded to either oxygen or silicon atoms. This structure is simulated by the generalized Bethe lattice model, where the Si–O and Si–Si bonds occur with the probabilities p and $1 - p$, respectively. Since the silicon and oxygen atoms are

**Fig. 1.** (Dashed line) Total charge on silicon atoms, (horizontal straight lines) charges on silicon atoms in the v th tetrahedron, and (solid lines) charges on silicon atoms in the v th tetrahedron multiplied by the probability of the existence of this tetrahedron in SiO_x versus x .**Table 2.** Diagonal matrix elements of the Hamiltonian

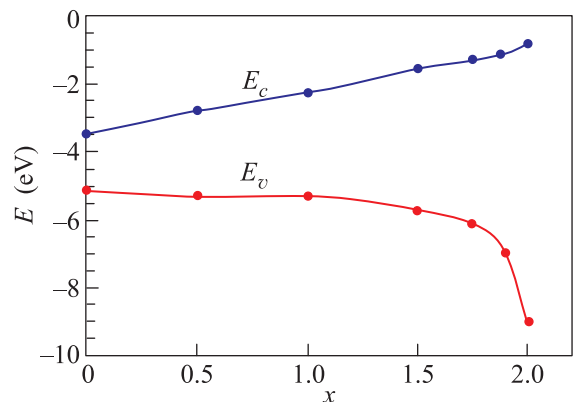
Atom	H_s^0/H_s	H_p^0/H_p	$H_{s^*}^0/H_{s^*}$
Si	-14.79/-8.301	-8.08/-1.701	-3.11/-3.269
O	-33.85/-26.233	-17.19/-9.573	-7.94/-0.323

four- and twofold coordinated, respectively, SiO_x can be represented as a set of random $\text{Si}-\text{Si}_v\text{O}_{4-v}$ tetrahedra with a Si atom at the center of a tetrahedron, where $v = 0-4$ is the number of Si–Si bonds and $4 - v$ is the number of Si–O bonds in the v th tetrahedron. The distribution of such tetrahedra satisfies a binomial law

$$W_v(p) = C_4^v p^{(4-v)}(1-p)^v. \quad (9)$$

In this model, the probability is $p = x/2$ and varies from 0 to 1 at the $\text{Si} \rightarrow \text{SiO}_2$ transition.

The generalized Bethe lattice model partially involves closed rings of bonds between sites of the lattice and, in combination with the tight-binding method, is used to model the electronic structure of disordered media (e.g., [17]). As was shown in [13], the topology of the generalized Bethe lattice imitates well the disordered topology of bond rings in amorphous structures at the calculation of features in the energy density of states. In particular, in the generalized Bethe lattice model, the centers of gravity of bands are not displaced, and the charge filling of energy bands, as well as the local partial density of states, i.e., occupation numbers appearing in Eqs. (7) and (8), is not redistributed. Consequently, the generalized Bethe lattice model can reliably be used to calculate the charge state of atoms of the lattice and the matrix elements of the tight-binding Hamiltonian. The charge state of silicon atoms Q in units of the elementary charge $|e|$ calculated with the data presented in Table 2 is shown in Fig. 1 as a function of the oxygen content in SiO_x .

**Fig. 2.** (Color online) Energy diagram of SiO_x at the $\text{Si} \rightarrow \text{SiO}_x \rightarrow \text{SiO}_2$ transition.

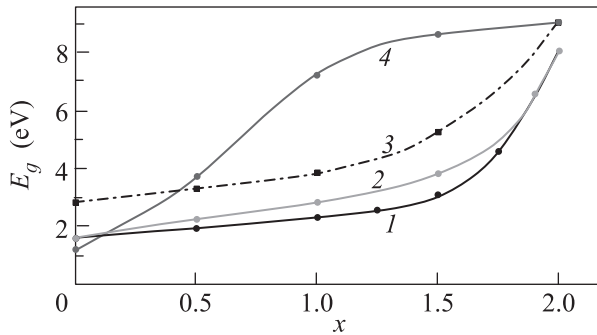


Fig. 3. Width of the band gap in SiO_x at the $\text{Si} \rightarrow \text{SiO}_x \rightarrow \text{SiO}_2$ transition versus x according to (1) experiment [22], (2) our calculation, (3) [10], and (4) [9].

We verified the parameters used in the calculation of the electronic structure of SiO_x by calculating the well-known parameters of the electronic structure of SiO_x with $x = 0$ and 2, i.e., for silicon and silicon oxide, respectively. The results of this calculation are presented in Table 3 in comparison with the results from [12, 13] and with experimental data. According to Table 4, our results are significantly closer to the experimental data than the results obtained in [12, 13].

The x dependence of the positions of the bottom of the conduction band E_c and the top of the valence band E_v is shown in Fig. 2. Figure 2 demonstrates a characteristic kink of E_v at $x \approx 1.75$. This x value is close to the percolation threshold in amorphous structures. K. Hubner [12] was the first who noted this circumstance, but the threshold x value in his work fell within the range of 1.25–1.5. This value differs from

Table 3. Calculated and experimental widths of the band gap E_g and the position of the top of the valence band E_v in silicon and silicon oxide

Parameter	Material	This work	[9]	[10]	Experiment [4]
E_v	Si	-5.15	6.9	-4	-5.2
	SiO_2	-8.97	-10.0	-10.5	-9.0
E_g	Si	1.6	1.2	2.94	1.6
	SiO_2	8.0	9.0	9.5	8.0

Table 4. Calculated and experimental of barrier heights for the injection of electrons and holes in SiO_2

Φ (eV)	This work	Experiment [4]
Φ^e (eV)	2.58	2.6
Φ^h (eV)	3.85	3.8

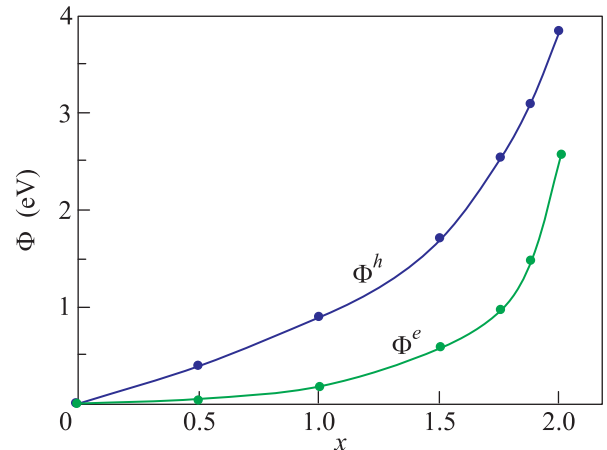


Fig. 4. (Color online) Height of the barrier Φ for electrons $\Phi^e = E_c(x) - E_c(0)$ and holes $\Phi^h = E_v(0) - E_v(x)$ in SiO_x versus x .

our results possibly because Hubner developed a qualitative theory in [12].

The x dependence of the width of the band gap E_g is shown in Fig. 3 in comparison with the previous calculations [9, 13] and experiment [25]. It is seen in Fig. 3 that our calculation is in better agreement with experimental data than the previous calculations.

The calculated heights of the energy barriers for electrons Φ^e and holes Φ^h are shown in Fig. 4.

Table 4 presents the calculated and experimental heights of barriers for the injection of electrons Φ^e and holes Φ^h in SiO_2 .

To summarize, the energy barriers for the injection of electrons and holes from silicon to SiO_x have been calculated for the first time. It has been shown that a change in the localization region of valence electrons in silicon and oxygen atoms plays an important role in the formation of the electronic structure of SiO_x . Taking into account this change, the electronic structure of silicon-enriched SiO_x as a function of the degree of enrichment has been calculated by the ab initio tight binding method within the generalized Bethe lattice model without any fitting procedures. The charge state of silicon and oxygen atoms has been determined as a function of the degree of silicon enrichment in silicon oxide. The width of the band gap of SiO_x has been determined as a function of x . The results are in good agreement with experimental data.

This work was supported by the Russian Foundation for Basic Research (project no. 17-02-01827), the Russian Science Foundation (project no. 18-49-08001), and the Ministry of Science and Technology of Taiwan (MOST grant no. 107-2923-E-009-001-MY3).

REFERENCES

1. T. V. Perevalov and V. A. Gritsenko, Phys. Usp. **53**, 561 (2010).
2. N.-M. Park, S. H. Kim, G. Y. Sung, and S.-J. Park, Phys. Rev. Lett. **86**, 1355 (2001).
3. J. Borghetti, G. S. Snider, Ph. J. Kuekes, J. J. Yang, D. R. Stewart, and R. S. Williams, Nature (London, U.K.) **464**, 873 (2011).
4. V. A. Gritsenko and D. R. Islamov, *Physics of Dielectric Films: Mechanisms for Charge Transport and Physical Principles of Memory Devices* (Parallel', Novosibirsk, 2017), p. 352 [in Russian].
5. M.-J. Lee, Ch. B. Lee, D. Lee, S. R. Lee, M. Chang, J. H. Hur, Y.-B. Kim, Ch.-J. Kim, D. H. Seo, S. Seo, U-In Chung, In-K. Yoo, and K. Kim, Nat. Mater. **10**, 625 (2011).
6. J. Yao, Zh. S. L. Zhong, D. Natelson, and J. M. Tour, Nano Lett. **10**, 4105 (2010).
7. G. Wang, Y. Yang, J. H. Lee, V. Abramova, H. Fei, G. Ruan, and E. L. Thomas, Nano Lett. **14**, 4694 (2014).
8. A. Mehonic, M. Buckwell, M. Bosman, and A. L. Shluger, Adv. Mater. **28**, 7486 (2016).
9. H. M. Kittur and A. Chin, Sci. Rep. **7**, 42375 (2017).
10. K. A. Nasyrov, S. S. Shaimeev, and V. A. Gritsenko, J. Exp. Theor. Phys. **109**, 785 (2009).
11. K. A. Nasyrov and V. A. Gritsenko, Phys. Usp. **56**, 999 (2013).
12. K. Hubner, J. Non-Cryst. Solids **36**, 1011 (1980).
13. E. Martinez and F. Yndurain, Phys. Rev **24**, 5718 (1981).
14. M. V. Ivanov, T. V. Perevalov, V. Sh. Aliev, V. A. Gritsenko, and V. V. Kaichev, J. Exp. Theor. Phys. **112**, 1035 (2011).
15. V. A. Svets, V. Sh. Aliev, D. V. Gritsenko, S. S. Shaimeev, E. V. Fedosenko, S. V. Rykhllitski, V. V. Atuchin, V. A. Gritsenko, V. M. Tapilin, and H. Wong, J. Non-Cryst. Solids **354**, 3025 (2008).
16. T. V. Perevalov, V. A. Gritsenko, S. B. Erenburg, A. M. Badalyan, H. Wong, and C. W. Kim, J. Appl. Phys. **101**, 053704 (2007).
17. A. A. Karpushin, A. N. Sorokin, I. Yu. Semenova, and M. Tomashek, Phys. Status Solidi B **136**, 331 (1986).
18. A. N. Sorokin, A. A. Karpushin, V. A. Gritsenko, and H. Wong, J. Non-Cryst. Solids **354**, 1531 (2008).
19. A. N. Sorokin, A. A. Karpushin, V. A. Gritsenko, and H. Wong, J. Appl. Phys. **105**, 073706 (2009).
20. A. N. Sorokin, A. A. Karpushin, and V. A. Gritsenko, JETP Lett. **98**, 709 (2013).
21. A. A. Karpushin, A. N. Sorokin, and V. A. Gritsenko, JETP Lett. **103**, 171 (2016).
22. W. A. Harrison, Phys. Rev. B **31**, 2121 (1982).
23. W. A. Harrison, *Electronic Structure and the Properties of Solids* (Freeman, San Francisco, 1980).
24. M. I. Shaskol'skaya, *Crystallography* (Vysshaya Skola, Moscow, 1976) [in Russian].
25. E. Holzenkampfer, F. W. Richter, J. Stuk, and U. Vogel-Grote, J. Non-Cryst. Solids **32**, 327 (1979).

Translated by R. Tyapaev

SPELL: OK